

# Efficient Electrochemical Degradation of Malachite Green Using Fluorine Doped Tin Oxide (FTO) Conductive Glass as Anode

Yiting Chen<sup>1,2,\*</sup>, Dechun Fan<sup>3</sup>, Lu Huang<sup>1,2</sup>, Yanxia Li<sup>1,2</sup>, Zhenli Qiu<sup>1,2</sup>, Chen Feng<sup>4,\*</sup>

<sup>1</sup> Ocean College, Minjiang University, Fuzhou, Fujian 350108, China;

<sup>2</sup> Fujian Provincial University Engineering Research Center of Green Materials and Chemical Engineering (Minjiang University), Fuzhou, Fujian 350121, China;

<sup>3</sup> College of Materials Science and Engineering, Fuzhou University, Fuzhou, Fujian 350108, China;

<sup>4</sup> Key Laboratory of Green Energy and Environment Catalysis (Ningde Normal University), Fujian Province University, 350002, China

\*E-mail: [fjcyt@foxmail.com](mailto:fjcyt@foxmail.com) (Dr. Y.T. Chen), [chenfeng710828@163.com](mailto:chenfeng710828@163.com) (Dr. F. Chen).

Received: 26 May 2020 / Accepted: 26 August 2020 / Published: 30 September 2020

---

The malachite green (MG) has been widely used in the aquaculture and textile industry as drugs and dyes, respectively. In recent years, it has been found that MG has side effects such as carcinogenicity, teratogenicity and mutagenesis. So it becomes particularly important to degrade MG for these industries. In this paper, a set of equipment using FTO conductive glass was developed for degradation of MG. Several factors affecting the efficiency of electrochemical degradation, including the solution of pH, electrolyte, applied current density and degradation time were investigated. Based on the results of single-factor experiment, the response surface methodology (RSM) was used for optimal conditions. The degradation rate of MG reaches above 98% by electrolysis in 6.56 g/L NaCl (pH 8.84) solution with current density as 8.61 mA/cm<sup>2</sup> for 20 min. The degradation process was preliminarily investigated by ultraviolet-visible(UV-vis) spectroscopy, fluorescence spectrometry, and total organic carbon analysis. The equipment and operation is simple, therefore could be used for the degradation of wastewater yielded during production.

---

**Keywords:** malachite green; electrochemical; degradation; FTO

## 1. INTRODUCTION

Malachite green (MG) is a synthetic triphenylmethane industrial dye. It is not only used as dyes in the silk industry, textile industry and other industries, but also widely used as efficient vermifuges and antibacterial drugs in aquaculture. Its chemical functional group-triphenylmethane has carcinogenic, teratogenic, mutagenic and other side effects, and also has an impact on biological

tissues, reproductive and immune systems. If wastewater containing MG directly discharges into the natural environment, MG will enter into the ecological cycle, resulting in adverse effects. Therefore, it is imperative to study the degradation of MG.

The methods for the treatment of MG mainly include photocatalytic degradation [1-2], adsorption [3], biodegradation [4-5], photo Fenton [6-7], electrolysis [8-10], ultrasonic degradation [11], microwave degradation [12] and etc. Since electrochemical processing technologies have many advantages such as fast degradation rate, high removal rate of pollutants, low secondary pollution, they are known as the environmentally friendly technology and have a tremendous potential as a green technology.

Since the oxidative degradation of dyes mainly occurs at the anode, the anode material is the key factor affecting the efficiency and energy consumption of organic matter degradation [13-19]. Seeking electrode materials with good performance and easy obtainment is highly important for further improving the electrochemical degradation efficiency. In recent years, fluorine-doped SnO<sub>2</sub> transparent conductive glass (SnO<sub>2</sub>:F, FTO glass) with low surface resistance, high light transmittance, and low cost has been used as a novel anode material for the electrochemical degradation of dye solutions, and excellent results have been obtained [20-22]. To date, no correspondences are known to establish the optimization of degradation of MG by FTO glass.

Most of the studies conducted to date do not report the inter-action of all the independent variables used in the degradation studies. Response surface methodology (RSM) is a useful mathematical and statistical method for analyzing the relation between several independent variables and one or more responses [23-24]. In this thesis, based on the results of single-factor experiment, the RSM was applied to optimize the removal rate of MG.

In this work, FTO conductive glass was used as the electrode material to study the electrochemical degradation of MG simulation wastewater by applying the RSM, and the degradation behavior was further explored, which would provide a theoretical basis and application guide for the electrochemical degradation of MG wastewater in production.

## 2. EXPERIMENTAL

### 2.1 Reagents

Malachite green oxalate salt was purchased from Aladdin Industrial Corporation; Sodium chloride, sodium sulfate and potassium nitrate were obtained from China National Pharmaceutical Group Co., Ltd. (Sinopharm). All reagents were of analytical grade; ultra-pure water was used in the experiments (Milli-Q, Millipore, America).

### 2.2 Apparatus

A laboratory-built equipment using FTO glass was used in the experiment. The overall setup includes two sub-units was shown in Fig.1, an electrochemical degradation system and a real-time UV-vis detection. Two pieces of FTO glass ( $8 \Omega/\text{cm}^2$ , purchased from Dalian Heptachroma Solar Tech.

Co., Ltd., China) were used as the anode electrode material and the graphite electrode (purchased from Tianjin Aidahengsheng Technology Co., Ltd., China) as the cathode. FTO conductive glass was cut into the appropriate size, and then placed in a 20 cm glass groove. The glass groove was fixed in a dark chamber, and the dye solution was stirred by a magnetic stirrer. The degradation was performed under an appropriate current density, which was provided by WS-YL digital stabilized power supply (Nanjing Sangli Electronic Equipment Factory, China).

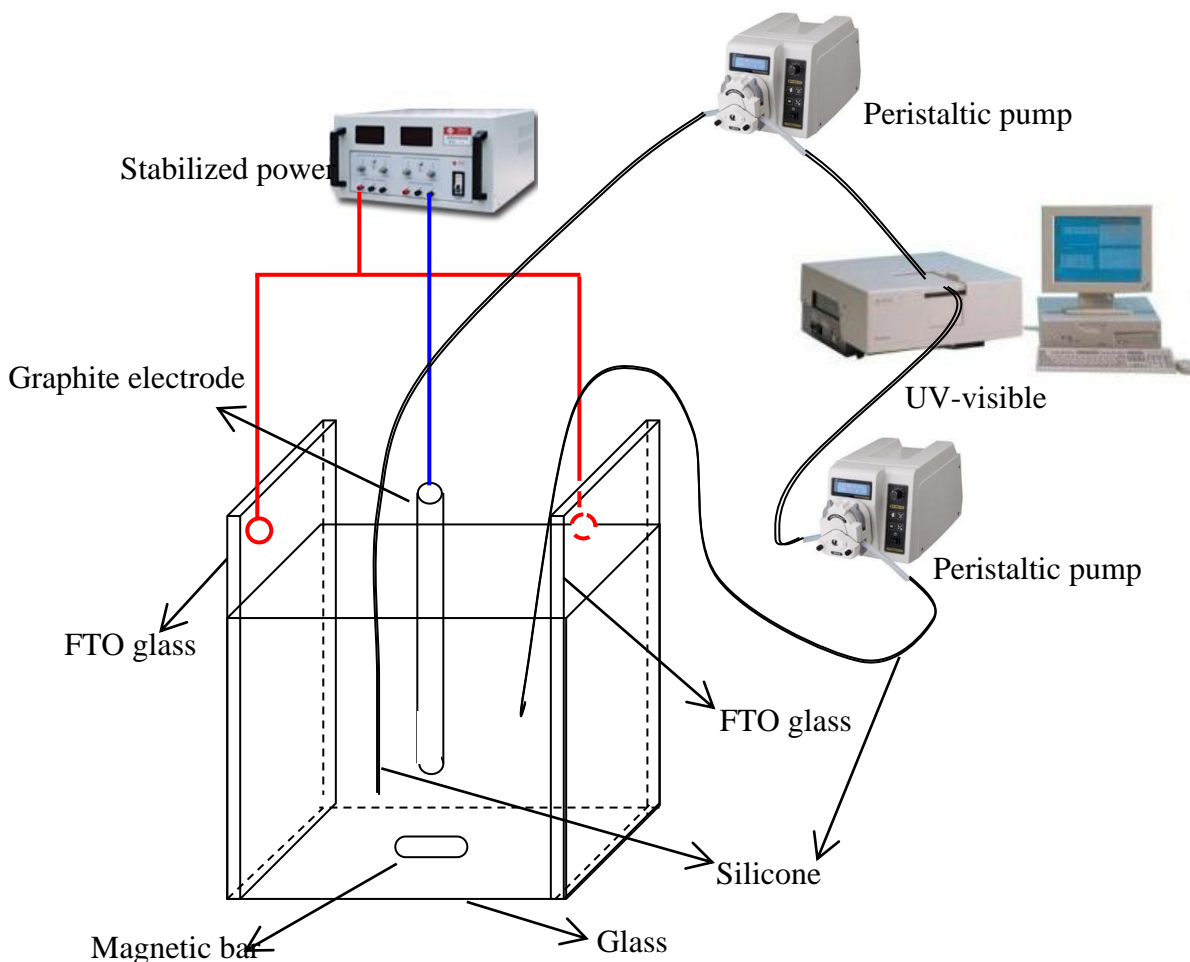


**Figure 1.** Schematic diagram of the reactor used for degradation of MG with FTO.

The dye solution in glass groove was passed through the ultraviolet-visible (UV-vis) spectrophotometer (UV-2550, Shimadzu, Japan) using two peristaltic pumps at the same flow rate, which in order to real-time monitor the changes in concentrations of MG solutions. To avoid the effect of environment light on the degradation of MG, all the experiments, including the electrical degradation process were performed in a darkroom with the room temperature controlled at 25 °C.

### 2.3 Determination of MG removal rate ( $\eta$ )

There are two mechanisms of MG electrochemical degradation, namely direct oxidation and indirect oxidation. In direct anodic oxidation, the MG are adsorbed on the anode surface and destroyed

by the anodic electron transfer reaction. However, the degradation of MG was mainly accounted for by the indirect oxidation in the liquid bulk which is mediated by the oxidants that are formed electrochemically; such oxidants include chlorine, hypochlorite and hydroxyl radicals. Anodic water discharge results in the formation of hydroxyl radicals, which could oxidize the MG[25-27],



In the presence of NaCl, chlorohydroxyl radicals are also formed on the anode surface and then oxidize the organic matter



At the same time, the cathode electrode reacts as Eqs. (5):



The residual quantity of MG during the degradation process could be obtained by measuring the absorbance of the MG solution at the wavelength of 618 nm and combining with the working curve. And the MG removal rate could be calculated by the following formula:

$$\eta\% = \frac{C_0 - C_1}{C_0} \times 100 \quad (6)$$

where  $\eta$  was the MG removal rate;  $C_0$  was the initial concentration of MG, mg/L;  $C_1$  was the residual concentration of MG, mg/L.

#### 2.4 Characterization of degradation products

MG solutions before and after 20 min of electrolysis were characterized using the following technologies: UV-vis spectrophotometer (UV-2550, Shimadzu, Japan) was used for measuring UV-vis absorption spectra between 200~700 nm; fluorescent spectrometry was used for the fluorescent scanning of solutions before and after electrolysis with the emission wavelength range between 300~500 nm and the excitation wavelength range between 250~350 nm by fluorescence spectrophotometer (F-380, Tianjin Gangdong Sci.&Tech. Development Co. Ltd., China); infrared spectrums of MG and degradation products were obtained by infrared spectrometer (Nicolet iS5, Thermo Fisher Scientific Inc, USA); total organic carbon (TOC) analysis was used for the determination of TOC and inorganic carbon (IC) of solutions before and after electrolysis by (TOC-V<sub>CPH</sub>, Shimadzu, Japan).

### 3. RESULTS AND DISCUSSION

#### 3.1 Absorption spectra of MG solution

Absorption spectra were obtained by measuring the absorbance of MG solution (1 mg/mL) at the wavelength range between 200~700 nm. As shown in Fig. 2, there were absorption peaks of MG solution at the wavelength of 618 nm, 423 nm and 343 nm. Among them, the peak at 618 nm was the strongest one. MG belongs to triphenylmethane dyes whose leuco bodies have two absorption peaks at

the wavelength of 260 and 300 nm, respectively. However, since the phenyl group of MG was an electron withdrawing group, its introduction caused the lowest unoccupied molecular orbital energy level descended. Hence, the maximum absorption wavelength of MG shifted towards the longer wavelength side. The absorption peak near 618 nm was the characteristic absorption peak of MG cations. After electrochemical degradation, all absorption peak of MG solution within the wavelength range between 250~700 nm disappeared. Therefore, the changes in the MG concentration could be characterized by monitoring the changes in the absorbance of the MG solution at the wavelength of 618 nm. In this way, the removal rate of MG could be obtained.

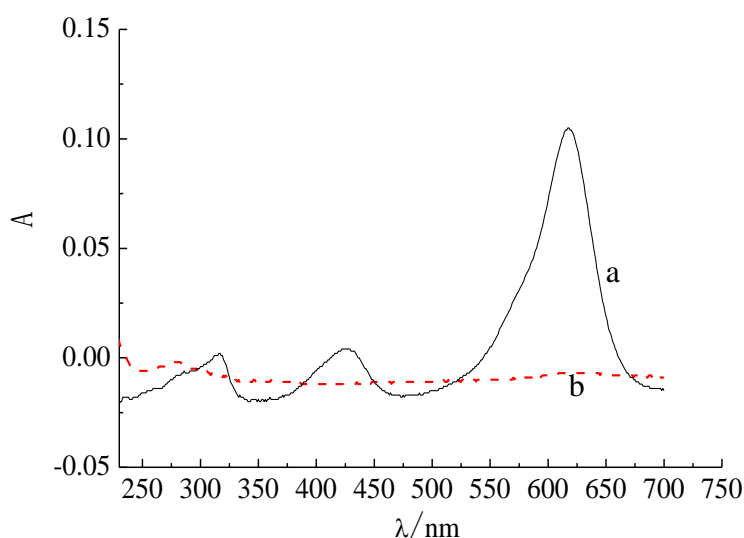


**Figure 2.** UV visible absorption spectra of MG solutions, a: before electrolysis; b: after electrolysis

A series of MG solutions with different concentrations were prepared, and their absorbance values were measured at the wavelength of 618 nm. The linear equation of the standard curve obtained was  $A=0.1530 \times C(\text{mg/L})-0.0387$  ( $R^2=0.9996$ ) with the linearity range between 0.5 to 15 mg/L.

### 3.2 Effect of pH on the MG removal rate

The pH value of the solution can affect the production and stability of hydroxyl radicals in the solution. Hence, the effect of pH on the MG removal rate was firstly investigated. An electrolytic current with a current density of  $8 \text{ mA/cm}^2$  was applied to an MG solution (10 mg/L) containing NaCl (6 g/L) with different pH for 30 min. The experimental results are shown in Figure 3.

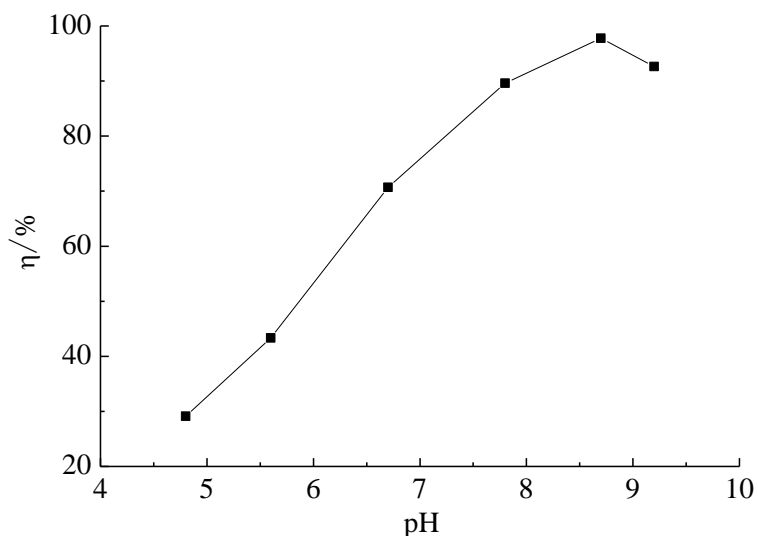


**Figure 3.** Effect of pH on the MG removal rate. Conditions: initial concentration of MG 10 mg/L; current density 8 mA/cm<sup>2</sup>; treatment time 30 min; concentration of NaCl 6 g/L.

As shown in Fig. 3, with the increase of pH, the MG removal rate first increased, then decreased at higher pH. This phenomenon might probably be related to the production of hydroxyl radicals. When the pH was 8.6, the MG removal rate was the best (more than 96%), then it declined by further increasing the pH. Besides, too alkaline and too acidic solutions can cause the corrosion of FTO conductive glass. Therefore, 8.6 was chosen as the solution pH.

### 3.3 Effect of electrolyte type on the MG removal rate

The effect of NaCl, KNO<sub>3</sub> and Na<sub>2</sub>SO<sub>4</sub> at the same concentration (6g/L) as electrolytes on the electrochemical degradation of MG solutions was investigated.

As shown in Fig. 4, within 10 min of degradation, the removal rate of KNO<sub>3</sub> as the electrolyte was the best, while those of NaCl was better after 10 min of degradation. Judging from the rate to reach the maximum removal rate, NaCl was faster than KNO<sub>3</sub> and Na<sub>2</sub>SO<sub>4</sub>. NaCl could oxidize to form chlorine and then hypochlorous acid. This might be related to the active chlorihydroxyl radicals are also formed on the anode surface in the presence of NaCl as follows[28-31]:



Although its oxidation effect is not as good as hydroxyl radicals, the HOCl/OCl<sup>-</sup> pair reacts with organic compounds by addition, substitution or oxidation[31-32], which could improve the

degradation efficiency of organic pollutants. Furthermore, considering the low cost of NaCl and the lowest consumption at the same concentration, NaCl was thus chosen as the electrolyte.

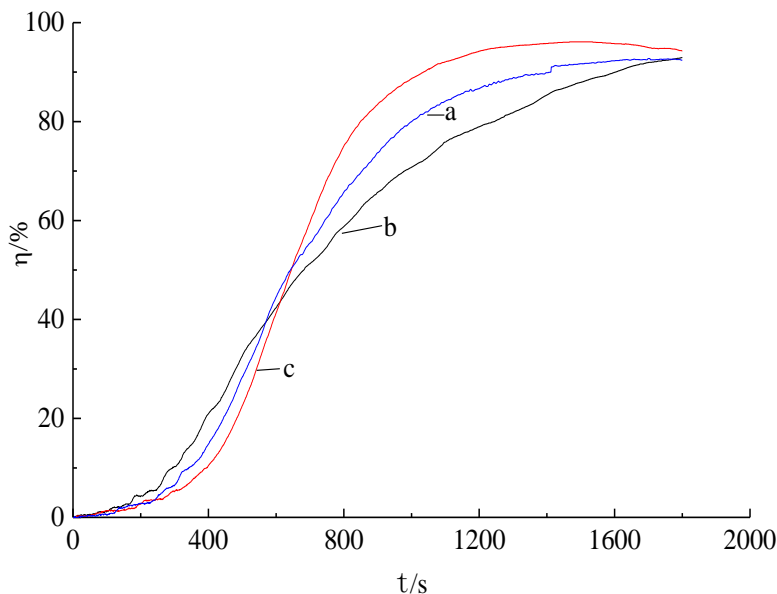


**Figure 4.** Effect of the electrolyte types on the MG removal rate. a: Na<sub>2</sub>SO<sub>4</sub>; b: KNO<sub>3</sub>; c: NaCl, Conditions: pH 8.6; electrolyte concentration 6 g/L; current density 8 mA/cm<sup>2</sup>; initial concentration of MG 10 mg/L.

### 3.4 Effect of electrolyte concentration on the MG removal rate

MG solutions (pH 8.6, 10 mg/L) containing 2, 4, 6, 8 and 10 g/L NaCl were prepared and electrochemically degraded with 8 mA/cm<sup>2</sup> as current density for 30 min. The results are shown in Figure 5.

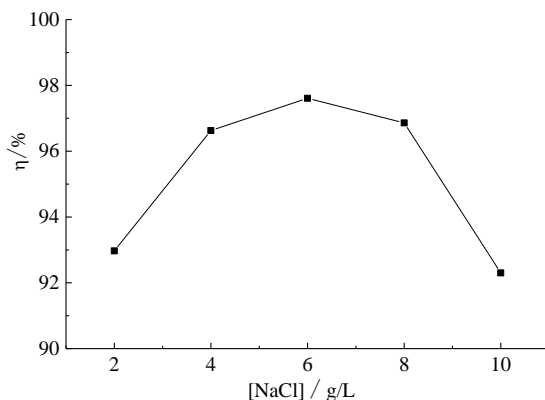


**Figure 5.** Effect of the electrolyte concentration on the MG removal rate. Conditions: pH 8.6; other conditions were the same as in Figure 3.

As shown in Fig. 5, with the increase of NaCl concentration, the MG removal rate first increased and then decreased. This might be due to the increased concentration of active chlorine and the increased conductivity of the solution, which resulted in the increase of the MG removal rate [32]. However, excessive NaCl affects the production of hydroxyl radicals in the solution [31], which resulted in the decrease of the MG removal rate. Therefore, 6 g/L was chosen as the NaCl concentration.

### 3.5 Effect of current density on the MG removal rate

Because of the close relationship between with the synergetic reactions of the most important species (hydroxyl radicals and active chlorine) and the current density [33-36], the effect of different current density on the degradation of MG (pH 8.6, 10 mg/L) was investigated.

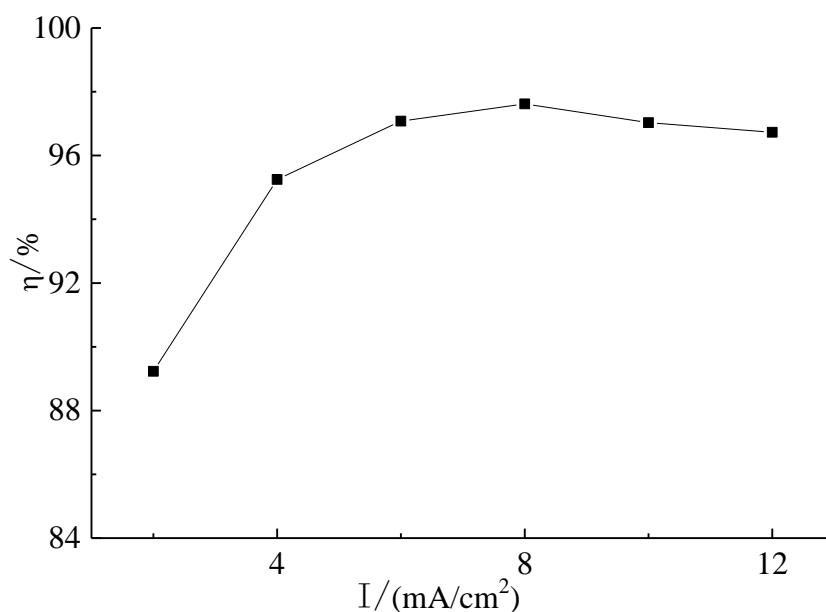


**Figure 6.** Effect of current density on the MG removal rate. Conditions: pH 8.6; other conditions were the same as in Figure 3.

The results (see Fig. 6) showed that with the increase of the current density, the MG removal rate first increased and then decreased. When the current density reached 8 mA/cm<sup>2</sup>, the MG removal rate achieved the highest. However, too much higher current density might cause side electrochemical reactions, which resulted in a decrease of the MG removal rate. Meanwhile, too much higher current density caused severe damage to FTO conductive glass. Therefore, 8 mA/cm<sup>2</sup> was chosen as the current density.

### 3.6 Effect of initial concentration of the MG solution on the MG removal rate

A series of MG solutions (pH 8.6, 6 g/L NaCl) at different concentrations were prepared to study the effect of MG concentration on the removal rate. The solution was electrolyzed at a current density of 8 mA/cm<sup>2</sup> for 20 min. The experimental results are shown in Figure 3.

As shown in Fig. 7 with the increase of the initial concentration, the MG removal rate first increased then decreased. When the concentration was above 10 mg/mL, the removal rate decreased. This might be because too much higher concentration caused part of MG undegraded. Considering the electrolytic efficiency, the concentration of MG solutions to be degraded was adjusted to 10 mg/L.

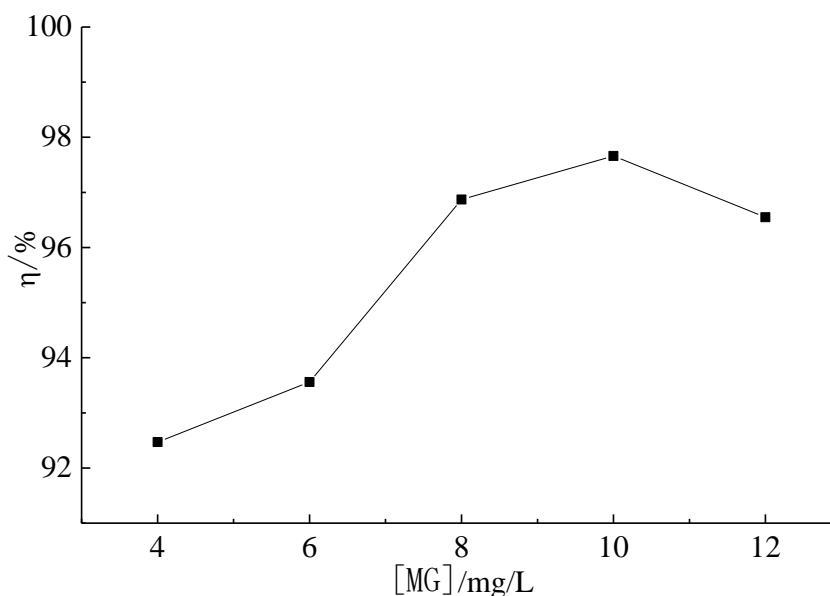


**Figure 7.** Effect of the initial concentration of the MG solution on the removal rate, Conditions: pH 8.6; other conditions were the same as in Figure 3.

### 3.7 Effect of treatment time on the MG removal rate

The real-time removal rate of MG solutions (pH=8.6, 6 g/L NaCl) at 10.0V was determined, and the results were shown in Fig. 8.

In the first 3 min, the removal rate increased slowly, which was related to fewer hydroxyl radicals and active chlorine in the solution. When the treatment time was between 3-20 min, the removal rate increased faster due to more and more hydroxyl radicals. When the treatment time was 20 min, most of MG was degraded. MG molecules on the electrode surface reduced, hence the removal rate value levelled off. This suggested that the removal rate reached its maximum. Therefore, 20 min was chosen as the treatment time with the removal rate up to 96%.

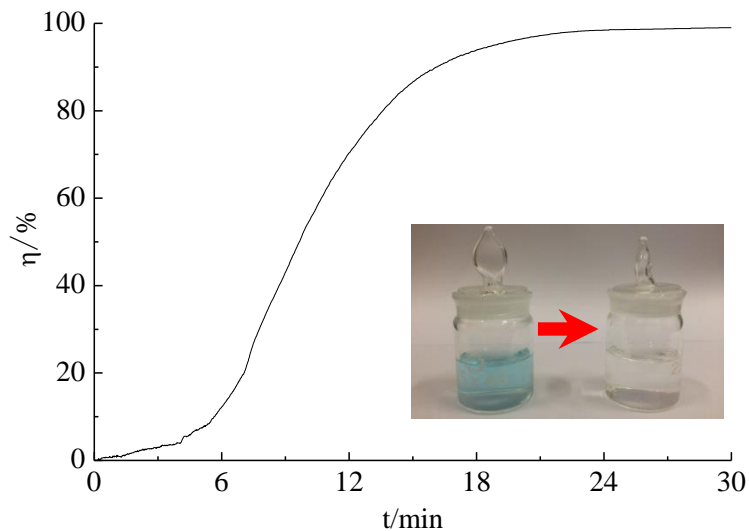


**Figure 8.** Effect of treatment time on the removal rate, Conditions: initial concentration of MG 10 mg/L; pH 8.6; current density 8 mA/cm<sup>2</sup>; degradation time 30 min; concentration of NaCl 6 g/L.

### 3.8 Analysis of RSM model

RSM is a sequential procedure with an initial objective to lead the experiments rapidly and efficiently along a path of improvement towards the general vicinity of the optimum. The Box-Behnken design for RSM was employed using Design-Expert Software Version 10. Based on the results of single-factor experiment, the influence of three parameters, such as pH, the concentration of NaCl ([NaCl]) and the current density (I), on the degradation rate was studied in RSM modeling. Each test was performed five times. The values recorded during the measurement are specific values of random variables; repeat measures have ensured of not being in the presence of an extreme value during the experiment. The results are shown in Table 1.

**Table 1.** Design and results of response surface analysis

Run	pH	[NaCl]/(g/L)	I/(mA/cm <sup>2</sup> )	η(%)	
				Actual Value	Predicted Value
1	10	8	8	85.48	84.97
2	10	6	4	76.21	76.63
3	10	4	8	78.28	77.95
4	9	6	8	96.13	96.90
5	9	6	8	96.55	96.90

6	9	6	8	97.71	96.90
7	9	6	8	97.23	96.90
8	8	8	8	89.06	89.39
9	9	4	4	82.71	82.62
10	9	4	12	93.58	93.49
11	8	6	12	88.79	88.37
12	10	6	12	82.87	83.29
13	8	4	8	87.31	87.82
14	9	8	4	93.10	93.19
15	9	6	8	96.88	96.90
16	9	8	12	91.41	91.50
17	8	6	4	86.26	85.84

**Table 3.** Analysis of variance for response surface quadratic regression equation

Source	Sum of Squares	Df	Mean Square	F Value	p-value Prob>F
Model	730.08	9	81.12	191.93	< 0.0001
pH	102.10	1	102.10	241.57	< 0.0001
[NaCl]	36.85	1	36.85	87.19	< 0.0001
I	42.18	1	42.18	99.80	< 0.0001
pH×[NaCl]	7.43	1	7.43	17.57	0.0041
pH×I	4.26	1	4.26	10.09	0.0156
[NaCl]×I	39.44	1	39.44	93.31	< 0.0001
pH <sup>2</sup>	361.63	1	361.63	855.60	< 0.0001
[NaCl] <sup>2</sup>	28.46	1	28.46	67.34	< 0.0001
I <sup>2</sup>	70.78	1	70.78	167.46	< 0.0001
Residual	2.96	7	0.42		
Lack of fit	1.48	3	0.49	1.33	0.381
Pure error	1.48	4	0.37		
Total	733.04	16			

Table 2 shows that the results of the RSM fitting of the experimental data set in the form of analysis of variance (ANOVA). The Model F-value of 65.18 implies the model is significant. In this case, pH, [NaCl], I, pH×[NaCl], [NaCl]×I, pH<sup>2</sup>, [NaCl]<sup>2</sup> and I<sup>2</sup> for the decolorization rate were found

to be extremely significant, which is evident from their Prob.>F value less than 0.01. pH×I was significant model term with Prob.>F value less than 0.05.

The numerical optimization analysis was operated by Design-Expert 10. The model equation for the removal rate in terms of actual factors was given as Eqs. (11).

$$\eta = -635.91375 + 157.09000 \times \text{pH} + 5.88188 \times [\text{NaCl}] + 4.70594 \times I + 0.68125 \times \text{pH} \times [\text{NaCl}] + 0.25813 \times \text{pH} \times I - 0.39250 \times [\text{NaCl}] \times I - 9.26750 \times \text{pH}^2 - 0.65000 \times [\text{NaCl}]^2 - 0.25625 \times I^2 \quad (11)$$

Based on the analysis above, the highest removal rate could be obtained, when the MG solutions (pH 8.84) containing 6.56 g/L NaCl was electrochemically degraded for 20 min with current density of 8.61 mA/cm<sup>2</sup>. Repeating this experiment for ten times, the average of the removal rate obtained was 98.05%, which was close to the predicted value (97.67%). It shows that the regression data matched the experimental data satisfactorily.

Compared with traditional chemical degradation, the proposed method uses neither chemical oxidizing nor reducing agent, and has low treatment cost and no secondary pollution. In addition, the method uses no photocatalytic reagent, Fenton reagent or other substances forming Fenton reagent, so that the cost is low and no separation and recovery of catalytic or Fenton reagents are needed after treatment. Compared with conventional anodes for MG removal[37-39], the FTO conductive glass can be obtained through commercialization without modification. A higher acidity is not required during the electrochemical degradation process, which avoids the problem that the treated wastewater should be neutralized before being expelled[40-41]. Besides, the equipment and operation in this proposed method is simple, therefore could be used for the degradation of wastewater yielded during production.

### 3.9 Analysis of the degradation behavior of MG

Taking tertiary butanol as the radical inhibitor, the effect of it on the MG removal rate was investigated. As shown in Fig. 9, with the increasing quantity of tertiary butanol added, the degradation of MG was inhibited much more, and the degradation rate became lower, which indicated that hydroxyl radicals played an important role in the degradation process [42-45]. The degradation of MG should mainly owe to the synergistic action of hydroxyl radicals and chlorine.

As displayed in Fig. 2, for MG before degradation, there were absorption peaks at the wavelength of 618 nm, 423 nm and 343 nm, among which the peak at 618 nm was the characteristic absorption peak of MG cations. After electrochemical degradation, the absorption peaks of MG in the visible light region almost disappeared, which indicated that chemical bonds of MG were damaged so that electrochemical degradation products had no absorption in the near-ultraviolet and visible light region. As the metabolite of MG in vivo, leucomalachite green leaves more hazardous than MG.

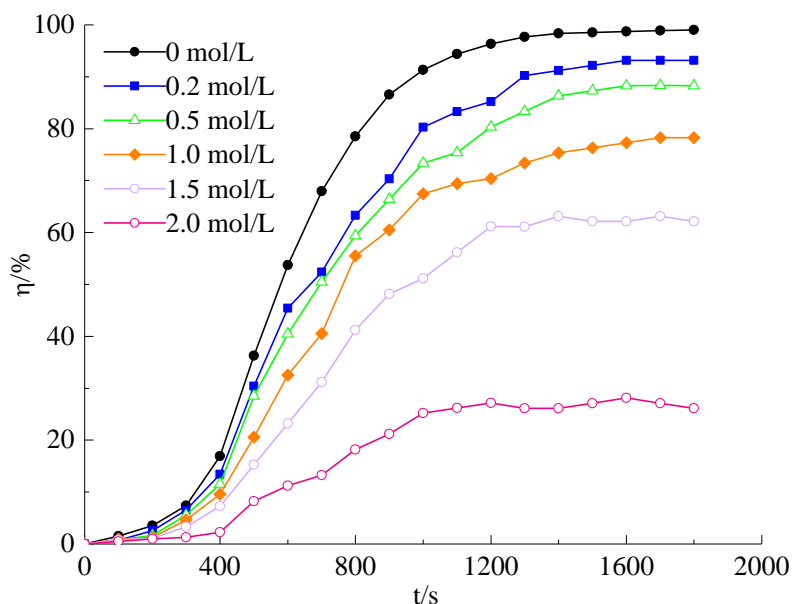


**Figure 9.** Effect of tertiary butanol on the removal rate

The maximum absorption wavelength of leucomalachite green was 260 nm [46], while MG solutions after degradation had no absorption here in Fig.2. Therefore, it could be asserted that there was no leucomalachite green in the solutions after electrochemical degradation.

Fluorescence analysis was made for the MG solutions before and after electrolysis (see Fig. 10). It was found that MG solutions before degradation had no obvious fluorescence, while MG solutions after electrochemical degradation had a strong fluorescence signal. First, the excitation wavelength was fixed at 303 nm; the fluorescence signal was measured at an emission wavelength range between 350~500 nm (Fig. 10A). It was observed that MG solutions before electrolysis had no obvious fluorescence signal, while MG solutions after electrolysis had a maximum fluorescence signal at 412 nm. Then, the emission wavelength was fixed at 412 nm; the fluorescence signal was measured at an excitation wavelength range between 250~350 nm (Fig. 10B). As displayed in Fig. 10B, MG solutions before electrolysis showed the weak fluorescence signal, whose maximum located at 303 nm. MG solutions after electrolysis had an obvious fluorescence signal and the optimum excitation wavelength shifted to 308 nm. It could be asserted that the structure of MG had changed. The maximum excitation wavelength of leucomalachite green is 265 nm, and the maximum emission wavelength is 360 nm [20]. This was inconsistent with the experimental results here. Therefore, it could be deduced that the degradation product of MG by this method was not leucomalachite green.

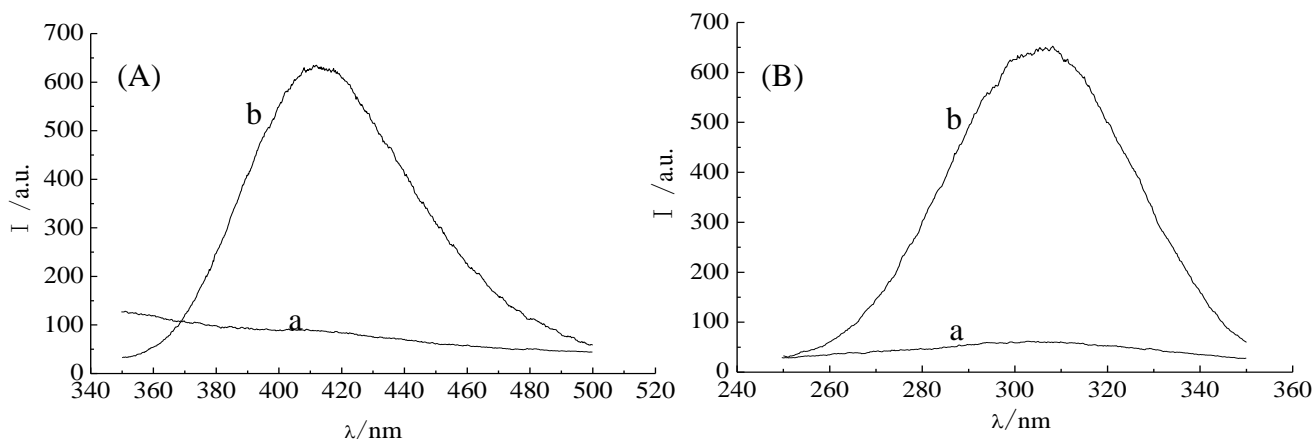


**Figure 10.** Fluorescence emission spectra of MG solutions before and after electrolysis, A, emission spectra; B, excitation spectra. a: MG; b: electrolysis remnants

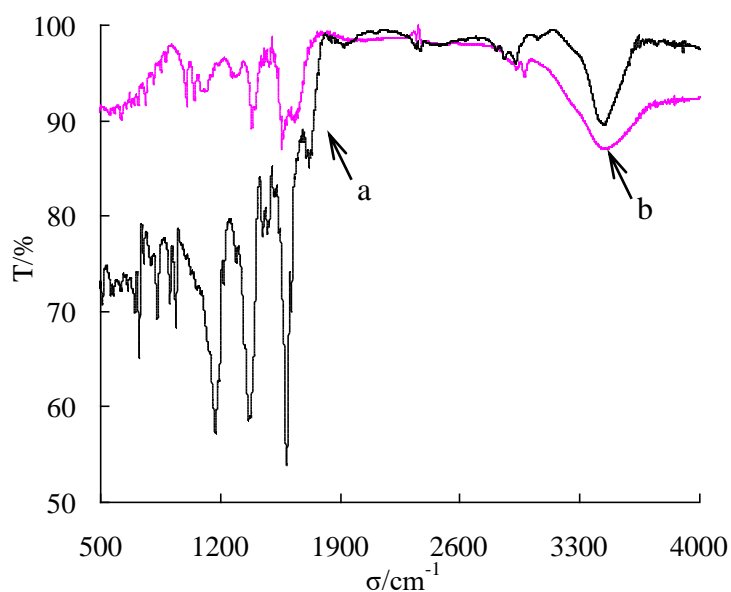


**Figure 11.** IR spectrum of MG and electrolysis remnants, a: MG; b: electrolysis remnants

The infrared spectrums of MG and degradation products were showed in Fig. 11. As shown by curve a in Fig. 11, the strong absorbance between 3400-3500  $\text{cm}^{-1}$  is the characteristic spectrum of -OH group on the oxalate. The peak at 1614  $\text{cm}^{-1}$  is due to the skeletal vibrations of the benzene ring. The peak at 1505  $\text{cm}^{-1}$  is associated with the stretching vibrations of C=C on the benzene ring. The peak in the vicinity of 1363  $\text{cm}^{-1}$  is assigned to -CH<sub>3</sub>. The peaks between 600-1000  $\text{cm}^{-1}$  is due to the out-plane bending vibration of C-H on the unsaturated carbon of olefin. After electrolysis, the IR absorption peaks of some groups disappeared or become weakened (curve b), which indicates that the chromophoric group of the dye molecule could be degraded after the electrolytic treatment.

TOC and IC of MG solutions before and after electrochemical degradation were determined. It was found that TOC decreased to 35.58% after 20 min electrochemical degradation. This indicated that

the structure of MG changed after electrochemical degradation, and most of the organic carbon turned into inorganic carbon.

The concentration of MG ( $C_{MG}$ ) at different time could be calculated by the linear equation of MG and the absorbance value at different time. When curves were made according  $C_{MG}$ ,  $\ln C_{MG}$ ,  $1/C_{MG}$  to the degradation time (t), it was found that  $\ln C$  was in a good linear relationship with t. The linear equation was  $\ln C_{MG} = -0.0032 \times t + 3.0798$ . Therefore, it could be deduced that the electrochemical degradation of MG was a first order process.

#### 4. CONCLUSION

A novel way using FTO conductive glass for the electrochemical degradation of MG was proposed. The pH and electrolyte of solution, current density and other influencing factors were studied. When the MG solutions (pH 8.84) containing 6.56 g/L NaCl was electrochemically degraded for 20 min with current density of 8.61 mA/cm<sup>2</sup>, the MG removal rate could reach up to 98%. In addition, the degradation behavior of MG was discussed. It was found that the electrochemical degradation of MG was a first-order process. The electrochemical degradation mechanism of MG on FTO conductive glass would be further explored using mass spectrum or other characterization techniques.

#### ACKNOWLEDGEMENT

This project was financially supported by NSFC (21405075), Program for New Century Excellent Talent of University in Fujian Province (2018), Fujian Province Natural Science Foundation (2019J01757), Key Laboratory of Green Energy and Environment Catalysis (Ningde Normal University) Research Fund(FJ-GEEC201805), Fuzhou science and technology project (2018-S-112), Science and technology project of Minjiang University (MYK17008, MYK18008, MYK19022).

#### References

1. S. Saha, J. M. Wang and A. Pal, *Separation and Purification Technology*, 89(2012) 147.
2. N. Arsalani, Y. Panahian and R. Nasiri, *Materials Science & Engineering B*, 251(2019)114448.
3. F. Y. Du, L. S. Sun, Z. J. Huang, Z. Y. Chen, Z. G. Xu, G. H. Ruan and C. X. Zhao, *Chemosphere*, 239(2020) 124764.
4. A. N. Kagalkar, M. U. Jadhav, V. A. Bapat and S. P. Govindwar, *Bioresource Technology*, 102(2011) 10312.
5. Z. G. Nejad, S. M. Borghei and S. Yaghmaei, *International Journal of Environmental Science and Technology*, 16(2019)7805.
6. H. L. Zheng, D. J. Peng, H. Li, X. H. Li, B. X. Wang and L. G. Xie, *Spectroscopy and spectral analysis*, 27(2007) 1006.
7. A. Ikhlaq, F. Javed, M. S. Munir, S. Hussain, K. S. Joya, and A. M. Zafar, *Desalination and Water Treatment*, 148 (2019) 152.
8. Z. Lin, H. Chen, Y. Zhou, N. Ogawa and J. M. Lin, *Journal of Environmental Sciences*, 24(2012) 550.
9. J. H. Yin, B. K. Xia, L. Du and S. G. Xiang, *Ekoloji*, 28( 2019)797.
10. S. Hanumanthappa, M. Shivaswamy and S. Mahesh, *Desalination and Water Treatment*, 146 (2019)

85.

11. Q. F. Zhuo, B. Yang, S. B. Deng, J. Huang, B. Wang and G. Yu, *Progress in Chemistry*, 24(2012) 628.
12. Y. M. Ju, S. G. Yang, Y. C. Ding, C. Sun, C. G. Gu, Z. He, C. Qin, H. He and B. Xu, *Journal of Hazardous Materials*, 171(2012)123.
13. H. A. Yusuf, Z. M. Redha, S. J. Baldock, P. R. Fielden and N. J. Goddard, *Microelectronic Engineering*, 149 (2016)31.
14. Z. Z. Li, C. S. Shen, Y. B. Liu, C. Y. Ma, F. Li, B. Yang, M. H. Huang, Z. W. Wang, L. M. Dong and S. Wolfgang, *Applied Catalysis B: Environmental*, 260(2020)118204.
15. E. Rafiee, N. Pami, A. A. Zinatizadeh and S. Eavani, *Journal of Photochemistry & Photobiology A: Chemistry*, 386(2020)112145.
16. G. Fadillah, T. A. Saleh, S. Wahyuningsih, E. N. K. Putri, and S. Febrianastuti, *Chemical Engineering Journal*, 378(2019)122140.
17. Y. W. Yao, G. G. Teng, Y. Yang, B. L. Ren and L. L. Cui, *Separation and Purification Technology*, 227(2019)115684.
18. M. A. Ajeel, M. K. Aroua and W. M. A. W. Daud, *Electrochimica Acta*, 180(2015)22.
19. A. Alaoui, K. E. Kazemi, K. E. Ass, S. Kitane and S. E. Bouzidi, *Separation and Purification Technology*, 154(2015)281.
20. L. A. Goulart, S. A. Alves and L. H. Mascaro, *Journal of Electroanalytical Chemistry*, 839(2019)123.
21. C. R. Osterwald, T. J. McMahon and J. A. D. Cueto, *Solar Energy Material & Solar Cells*, 79(2003)21.
22. Y.T. Chen, L. Huang and Q. Lin, *Environmental Chemistry*, 30(2011)1871.
23. P. Hou, F. S. Cannon, C. Nieto-Delgado, N. R. Brown and X. Gu, *Chemical Engineering Journal*, 223(2013)309.
24. J. D. Wang, J. C. Yao, L. Wang, Q. W. Xue, Z. T. Hu and B. J. Pan, *Separation and Purification Technology*, 230(2020)115851.
25. H. Zhang, J. Wu, Z. Q. Wang and D. B. Zhang, *Journal of Chemical Technology & Biotechnology*, 85(2010)1436.
26. C. Berberidou, I. Poulios, N. P. Xekoukoulotakis and D. Mantzavinos, *Applied Catalysis B: Environmental*, 74(2007)63.
27. E. Chatzisyneon, N. P. Xekoukoulotakis, A. Coz, N. Kalogerakis and D. Mantzavinos, *Journal of Hazardous Materials*, 137(2006) 998.
28. L. Du, J. Wu, G. Y. Li, S. Qin and C. W. Hu, *Acta Chimica Sinica*, 64(2006)2486.
29. X. J. Zhou, W. Q. Guo, S. S. Yang, H. S. Zheng and N. Q. Ren, *Bioresource Technology*, 128(2013) 827.
30. M. Muruganathan, S. Yoshihara, T. Rakuma, N. Uehara and T. Shirakashi, *Electrochimica Acta*, 52(2007) 3242.
31. R. E. Palma-Goyes, F. L. Guzmán-Duque, G. Peñuela, I. González, J. L. Nava and R. A. Torres-Palma, *Chemosphere*, 81(2010)26.
32. H. N. Li, Y. J. Long, X. P. Zhu, Y. L. Tian and J. Ye, *Electrochimica Acta*, 246 (2017) 1121.
33. S. Hussain, H. Asghar, H. Sattar, N. Brown and E. Roberts, *Journal of Applied Electrochemistry*, 45 (2015) 611.
34. N. Mohan, N. Balasubramanian, C.A and Basha, E, *Journal of Hazardous Materials*, 147(2007) 644.
35. A. Thiam, I. Sirés, J.A. Garrido and E. Brillas, *Separation and Purification Technology*, 140 (2015) 43.
36. F. Zaviska and P. Drogui, *Journal of Applied Electrochemistry*, 42(2012) 95.
37. A. Ansari and D. Nematollahi, *Water Research*, 144(2018)462.
38. F. Guenfoud, M. Mokhtari and H. Akrou, *Diamond & Related Materials*, 46 (2014) 8.

39. A.A. Jalil, M.A.H. Satar, S. Triwahyono, H.D. Setiabudi, N.H.N. Kamarudin, N.F. Jaafar, N. Sapawe and R. Ahamad, *Journal of Electroanalytical Chemistry*, 701 (2013) 50.
40. I. M. S. Pillai and A. K. Gupta, *Journal of Electroanalytical Chemistry*, 762 (2016) 66.
41. A. B. Jennifer, G. R. Orlando, E. G. Abdellatif, J. R. V. Francisco, A. G. Luis and B. Enric, *Journal of Environmental Chemical Engineering*, 4(2016)2066.
42. S. Y. Lu, Y. Z. Liu, L. Feng, Z. G. Sun and L. Q. Zhang, *Environmental Science And Pollution Research*, 25(2018) 5086.
43. J. Liu, J. S. Ye, Y. F. Chen, C. S. Li and H. Ou, *Chemosphere*, 190(2018)225.
44. Q. Wang, X. H. Lu, Y. Cao, J. Ma, J. Jiang, X. F. Bai and T. Hua, *Chemical Engineering Journal*, 328(2017)236.
45. Q.H. Yi, L. J. Bu, Z. Shi and S. Q. Zhou, *Chemical Engineering Journal*, 302(2016)417.
46. S. Q. Ju, J. Deng, J. L. Cheng, N. Xiao, K. Huang, C. H. Hua, H. Q. Zhao, J. Xie and X. Z. Zhan, *Food Chemistry*, 185(2015)479.

© 2020 The Authors. Published by ESG ([www.electrochemsci.org](http://www.electrochemsci.org)). This article is an open access article distributed under the terms and conditions of the Creative Commons Attribution license (<http://creativecommons.org/licenses/by/4.0/>).